03,13

Thermoelectric properties of Y_2O_3@SmS and $(Y_xGd_{1-x})_2O_3$@SmS with a core-shell type nanostructure

© A.V. Sotnikov, V.V. Bakovets, I.Yu. Filatova

Nikolaev Institute of Inorganic Chemistry, Siberian Branch, Russian Academy of Sciences, Novosibirsk, Russia

E-mail: sotnikov@niic.nsc.ru

Received December 1, 2023
Revised December 1, 2023
Accepted January 18, 2024

The conditions for the synthesis of compounds based on rare earth elements (REE) of the compositions Y_2O_3@SmS, $(Y_{0.90}Gd_{0.10})_2O_3$@SmS and $(Y_{0.99}Gd_{0.01})_2O_3$@SmS were optimized with a core-shell type nanostructure. The optimization process consisted in finding the minimum times and optimal temperatures at each stage of synthesis to stabilize the phase of Y and Gd oxides, as well as complete conversion to SmS in the studied composites after successive stages of sulfidation and annealing of the initial precursors. The thermoelectric properties in the temperature range $T = 298-873$ K were studied and compared with the literature data for thermoelectric compounds based on REE. For connection $(Y_{0.99}Gd_{0.01})_2O_3$@SmS at $T = 873$ K, the values of the Seebeck coefficient $S = -94\,\mu$V/K, the resistivity $\rho = 17\,\mu\Omega \cdot$ m and the total thermal conductivity coefficient $\kappa_{tot} = 1.50$ W/m $\cdot$ K. The maximum achieved value of the thermoelectric ZT parameter for the connection $(Y_{0.99}Gd_{0.01})_2O_3$@SmS reaches values of $ZT = 0.56$ at $T = 873$ K, which is a promising result in comparison with other thermoelectrics based on rare earth elements

Keywords: REE oxides and sulfides, sol-gel synthesis, core-shell, topological reactions.

DOI: 10.61011/PSS.2024.02.57914.266

1. Introduction

The growing demand for electrical and mechanical energy requires optimizing the approaches to efficient energy management, as well as accelerating the search for new clean and renewable sources. One of the most promising approaches is the development of devices based on thermoelectric materials (TEMs) capable of converting thermal energy into electrical energy. The introduction of TEMs will make it possible to use the world energy resources more economically, as well as significantly improve the environmental situation [1–4]. Besides, the use of thermoelectric devices will make it possible to transfer to hybrid engines, which will significantly reduce carbon monoxide emissions into the atmosphere and increase energy efficiency [5,6]. Thus, the development of new and modernization of already known TEMs are an urgent solution to the problem of the efficiency increasing of thermoelectric devices [7–10].

The efficiency of the thermoelectric material is determined by the dimensionless thermoelectric ZT parameter according to the formula $ZT = S^2 \cdot T/\rho \cdot \kappa_{tot}$, where defining parameters such as the Seebeck coefficient S, resistivity ρ and thermal conductivity κ_{tot} depend on the specific material [11]. Considering the interdependence of various transport parameters, the development of thermoelectric materials with increased efficiency is a very challenging task. This generates interest in developing new strategies and searching for potential materials that can reveal broader aspects for the search for new thermoelectric devices [12,13].

Recently, much attention was paid to the study of materials based on rare earth metal (REM) chalcogenides [7,14–17], including compounds with increased defectiveness based on solid solutions of REM sulfides [18–20], For example, in the paper [19] it was possible to significantly reduce the thermal conductivity coefficient due to additional heat dissipation through deformations of the cation sublattice. In [18] the found thermoelectric parameters of ceramic samples γ-$D_{y0.8}Yb_{0.2}S_{1.5-y}$ have high Seebeck coefficient, as well as low electrical resistivity and thermal conductivity. This is due to an increase in the specific area of crystallite boundaries and the concentration of deformation stresses at semi-coherent crystallite boundaries. As a result, it was possible to achieve the maximum value of the thermoelectric ZT parameter among all known compounds based on rare earth elements: $ZT = 0.60$ at $T = 770$ K. Thus, the concept of regulating crystalline and defect structures by changing dimension, control of the chemical composition of defects, and changing the atomic order of compounds represents a new breakthrough in the development of next generation thermoelectric materials.

It is known that the main way to obtain high values of thermoelectric ZT parameter is to reduce the thermal conductivity coefficient κ_{tot} and resistivity ρ, and on the other hand, it is necessary to increase the Seebeck coefficient S [21–23]. From this point of view, a promising direction for further search seems to be the synthesis of ceramic high-temperature composites with nanostructure of type „core−shell“ based on oxides, oxosulfides and sulfides of rare earth metals [24]. These compounds are built according

to the guest-host principle, where the „guest" plays the role of a „phononic glass" with low thermal conductivity, and the „host" has a metallic type of conductivity and plays the role of an „electronic crystal" [8]. In the paper [14] compounds with nanostructure of the core-shell type were studied for the first time. The most promising values of thermoelectric parameters at the indicator $ZT = 0.48$ $(T = 773\,\mathrm{K})$ were obtained for the compound of composition $SmS@Y_2O_2S$. It was also shown that a further increase in the ZT parameter is possible by increasing the Seebeck coefficient while maintaining optimal values of electrical resistivity by optimizing the concentration in the sample Y_2O_3. Further studies [25] on the development of compounds with core-shell nanostructure allowed for a specific polyol sol-gel synthesis, which resulted in increase in the number of core-shell particles. Besides, in the resulting compound $Y_2O_3@SmS$ it was possible to significantly increase the absolute value of the Seebeck coefficient ($-40\,\mu$V/K at $T = 430\,\mathrm{K}$), which is approximately by two times greater compared to the same parameter for $SmS@Y_2O_2S$. Thus, composites with core-shell nanostructure based on samarium monosulfide and yttrium oxide of rare earth elements (REE) were considered as promising new thermoelectric materials.

In this paper, the compounds $Y_2O_3@SmS$, $(Y_{0.90}Gd_{0.10})_2O_3)@SmS$ and $(Y_{0.99}Gd_{0.01})_2O_3@SmS$ were selected as objects of study. The preparation of solid solutions of REE oxides in the „core" structure will allow the creation of additional defects and disorder in the lattice, which will further increase the Seebeck coefficient and reduce the thermal conductivity of the material. It seems that the combination of such features of the components can provide conditions for increasing the thermoelectric ZT parameter composite as a whole. Thus, the objectives of this paper are the synthesis of compounds $Y_2O_3@SmS$, $(Y_{0.90}Gd_{0.10})_2O_3@SmS$ and $(Y_{0.99}Gd_{0.01})_2O_3@SmS$ with core-shell nanostructure and study of their thermoelectric properties.

2. Experimental part

To synthesize nanostructured powders of compounds with core-shell structure the rare earth element compounds were used as initial reagents: gadolinium and yttrium nitrates $Gd(NO_3)_3 \cdot 5H_2O$, $Y(NO_3)_3 \cdot 5H_2O$, samarium acetylacetonate $Sm(acac)_3$, as well as sodium hydroxide NaOH, urea $(NH_2)_2CO$ and ammonium rhodanate NH_4SCN. The content of the main components in these reagents was no less than 99.9%. The ethylene glycol $C_2H_4(OH)_2$ of „chemically pure" grade was used as an organic solvent.

The synthesis procedure was carried out according to the scheme described in detail in the paper [25]. At the initial stage sol-gel synthesis was carried out using solutions of alkali NaOH and gadolinium and yttrium nitrates. As a result, solid solutions of hydroxides of compositions $Y_xGd_{1-x}(OH)_3$ $(x = 0.9, 0.99)$ and separately $Y(OH)_3$ were obtained. The resulting hydroxides were annealed in a muffle furnace for 1 h at 873 K to obtain REE oxides. Next, suspensions of the resulting nanopowders were prepared in ethylene glycol and precipitation of $Sm(acac)_3$ with solution of $(NH_2)_2CO$ using polyol sol-gel synthesis was carried out similarly to the method described in [25]. The resulting powders were annealed in a muffle furnace for 1 h at 873 K to obtain appropriate oxides. Thus, three compounds were synthesized with core-shell nanostructure of the compositions $Y_2O_3@Sm_2O_3$, $(Y_{0.90}Gd_{0.10})_2O_3@Sm_2O_3$, $(Y_{0.99}Gd_{0.01})_2O_3@Sm_2O_3$.

Using solid-phase synthesis with powders $Y_2O_3@Sm_2O_3$, $(Y_{0.90}Gd_{0.10})_2O_3@Sm_2O_3$, $(Y_{0.99}Gd_{0.01})_2O_3@Sm_2O_3$ and ammonium rhodanate NH4SCN using the method [26,27] the samples were obtained containing the phase of samarium polysulfide SmS_2 on the surface of the particles. The sulfidation process was carried out in ammonium thiocyanate vapors at $T = 633\,\mathrm{K}$ for 10 h in inert atmosphere. Next, the resulting powders were mixed with metallic samarium in a stoichiometric ratio and thoroughly mixed in an agate mortar, then placed in the induction furnace, and the resulting mixture was heated at $T = 1423\,\mathrm{K}$ for 1 h. As a result, compounds of the composition $Y_2O_3@SmS$, $(Y_{0.90}Gd_{0.10})_2O_3@SmS$ and $(Y_{0.99}Gd_{0.01})_2O_3@SmS$ were obtained. The obtained products with core-shell nanostructure were sintered by hot pressing in vacuum at $T = 1423\,\mathrm{K}$ for 2 h with force of 70 MPa. The resulting ceramic materials were used to study micro-, nano-, and defect structures, as well as thermoelectric properties.

The phase composition of the compounds was determined by powder diffractometry. X-ray diffraction analysis (XRDA) of the obtained polycrystals was carried out on Shimadzu XRD-7000 diffractometer (CuK_α-radiation, Ni filter, range $10-80° 2\theta$, step 0.03°, accumulation 2 s).

The morphology of compressed compounds with core-shell nanostructure was studied using high-resolution transmission electron microscopy (HRTEM) on JEOL JEM-2010 device operating at a voltage of 200 kV and resolution of 1.4 Å. Samples for TEM were prepared by grinding sintered ceramics in agate mortar, creating suspension in methanol, and spreading them onto a carbon perforated mesh. The molar ratio of elements in the compounds was determined using energy dispersive chemical analysis (EDA) on Hitachi TM3000 TableTop SEM unit with Bruker QUANTAX 70 EDS attachment.

The temperature dependences of the Seebeck coefficient S were measured in a sparse (5 Torr) helium atmosphere with samples placed between two copper contact pads. A temperature gradient of 5 K between the copper contacts was maintained using Thermodat−13K5 thermostat. The thermo-emf between copper contact pads was measured with Keysight 34465A digital voltmeter. Resistivity ρ was measured by Van der Pauw method. The electrical properties were studied in the temperature range 298−873 K. The errors in determining the values of Seebeck coefficient and resistivity of the samples are $\sim 5\%$.

The temperature conductivity coefficient (χ_T) of the studied samples was determined by the laser flash method

on automated LFA-457 unit (NETZSCH (Germany)) in atmosphere of high-purity argon (Ar 99.992 vol.%) in the temperature range 298−873 K. Heat capacity measurements were carried out using the reference standard Pyroceram 9606. A flat sample is irradiated from below with a short pulse of laser radiation (1.064 μm). The error in measuring the temperature conductivity coefficient for solid samples is 2−5% depending on temperature. The overall temperature conductivity coefficient κ_{tot} was calculated using the well-known equation $\kappa_{tot} = \chi_T DC_p$, where χ_T — temperature conductivity coefficient, C_p — heat capacity, D — density of ceramic material. The experimental values χ_T obtained by the laser flash method contain lattice and electron diffusion components.

3. Results and discussion

3.1. High resolution XRDA and TEM

Figure 1 shows the XRDA results for the obtained compounds Y_2O_3@SmS, $(Y_{0.90}Gd_{0.10})_2O_3$@SmS and $(Y_{0.99}Gd_{0.01})_2O_3$@SmS.

One of the important tasks of this paper was the optimization of the method for multi-stage synthesis of compounds. The optimization process consisted of searching for optimal temperatures and times at each stage of synthesis to stabilize the phase of oxides Y and Gd, as well as the complete conversion of the „shell" in SmS after successive stages of sulfidation and annealing. Thus, in the resulting compounds, yttrium and gadolinium oxides occupy the internal region of the particles — „core", on which surface layers of samarium monosulfide — „shell" are formed. Besides, as XRDA results showed, in this paper single-phase compounds without trace impurities of REE oxosulfides and sesquisulfides were synthesized. The formation of solid solutions of REE oxides in compounds was also identified $(Y_{0.90}Gd_{0.10})_2O_3$@SmS and $(Y_{0.99}Gd_{0.01})_2O_3$@SmS.

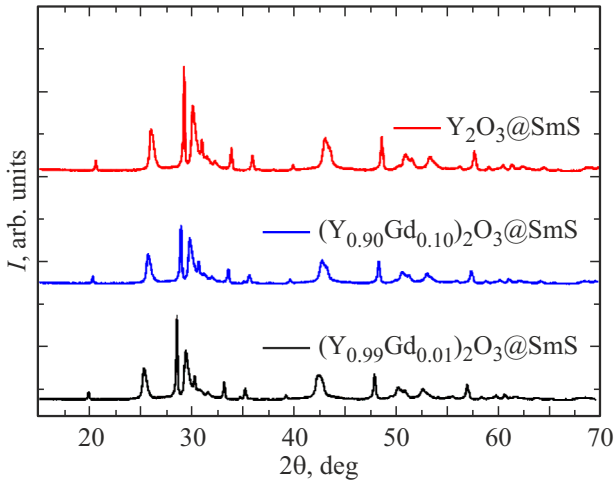

Figure 1. XRDA analysis of the obtained compounds Y_2O_3@SmS, $(Y_{0.90}Gd_{0.10})_2O_3$@SmS and $(Y_{0.99}Gd_{0.01})_2O_3$@SmS.

EDA results of compounds Y_2O_3@SmS, $(Y_{0.90}Gd_{0.10})_2O_3$@SmS and $(Y_{0.99}Gd_{0.01})_2O_3$@SmS

Sample	Content of element in sample, wt%				
	Sm	Gd	Y	O	S
Y_2O_3@SmS	37	–	43	12	8
$(Y_{0.90}Gd_{0.10})_2O_3$@SmS	36	7	38	11	8
$(Y_{0.99}Gd_{0.01})_2O_3$@SmS	37	1	43	11	8

Figure 2 shows the HRTEM results of the studied powders Y_2O_3@SmS, $(Y_{0.90}Gd_{0.10})_2O_3$@SmS and $(Y_{0.99}Gd_{0.01})_2O_3$@SmS. Experimental data confirmed the formation of a composite with core-shell nanostructure. Pre-obtained particles of oxides Y_2O_3, $(Y_{0.90}Gd_{0.10})_2O_3$ and $(Y_{0.99}Gd_{0.01})_2O_3$ have a plate-like shape. After the process of the core coating with $Sm(OH)_3$ shell, the core facet is smoothed. Thus, nanoparticles in the synthesis products Y_2O_3@SmS, $(Y_{0.90}Gd_{0.10})_2O_3$@SmS and $(Y_{0.99}Gd_{0.01})_2O_3$@SmS are characterized by a pronounced oval and hexagonal shape (Figure 2). The proposed sequence of synthesis routes promotes the formation of samarium oxide on the surface of REE oxides. However, the formation of individual particles Sm_2O_3 is not excluded. Thus, on the surface of the particle there is a darkened boundary of the core, like that of a heavier samarium atom (shown by arrows in Figure 2).

The study by HRTEM method allows us to conclude that the compounds contain a significant amount of „core-shell" nanoparticles. Optimization of the multi-stage synthesis of compounds made it possible to obtain particles with an average size of approximately 100−150 nm. The resulting value is by 30−50% lower compared to the particle sizes in the compounds Y_2O_2 S@SmS and SmS@Y_2O_2S obtained in [14]. This fact contributes to increase in the concentration of deformation centers and decrease in the thermal conductivity coefficient of the sintered ceramic sample [20].

The elemental composition of the studied samples correlates with the theoretical reference atomic concentration. The EDA results confirmed the ratio of Y, Gd, Sm, O and S atoms in the synthesis products Y_2O_3@SmS, $(Y_{0.90}Gd_{0.10})_2O_3$@SmS and $(Y_{0.99}Gd_{0.01})_2O_3$@SmS (see Table). Error of determination was $\sim$ 1%.

To analyze the effect of changes in the internal microstructure of compounds with core-shell nanostructure on their thermoelectric properties, it is necessary to determine correlations and relationships between the properties and the size of particles (crystallites). Taking into account the known features of changes in thermoelectric properties in compounds based on REE sulfides [18,19], associated with the morphology of powders and pressed ceramics, it can be assumed that similar processes will occur in the compounds under consideration with core-shell nanostructure.

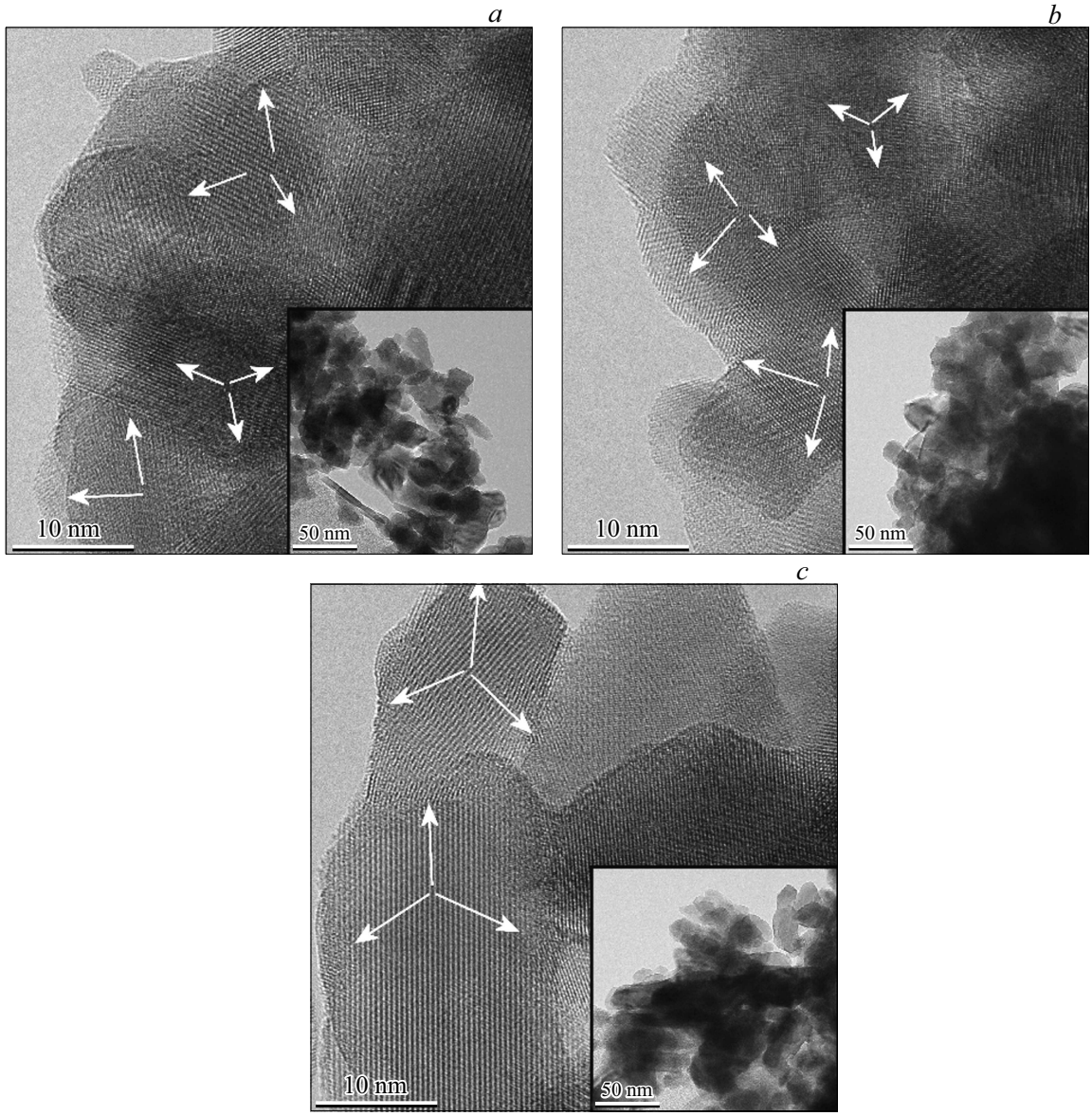

Figure 2. HRTEM results for compounds: *a* — Y_2O_3@SmS, *b* — $(Y_{0.90}Gd_{0.10})_2O_3$@SmS and *c* — $(Y_{0.99}Gd_{0.01})_2O_3$@SmS).

3.2. Thermoelectric properties

Figure 3 shows the temperature dependences of the Seebeck coefficient S (a), resistivity ρ (b) and power factor S^2/ρ (c) for compounds Y_2O_3@SmS, $(Y_{0.90}Gd_{0.10})_2O_3$@SmS and $(Y_{0.99}Gd_{0.01})_2O_3$@SmS. The obtained experimental dependences were compared with previously obtained results for compounds Y_2O_2 S@SmS and SmS@Y_2O_2S with core-shell nanostructure [14].

The negative sign of the Seebeck coefficient (Figure 3, a) indicates the electronic type (n-type) of conductivity in the resulting compounds. The temperature dependences of the parameter S change monotonically without obvious anomalies. The smallest value ($-94\,\mu$V/K) at $T = 873$ K is obtained for compound $(Y_{0.99}Gd_{0.01})_2O_3$@SmS. This is by $\sim 20\%$ lower then the same parameter for compound Y_2O_3@SmS and by $\sim 70\%$ lower then for the previously studied compounds Y_2O_2S@SmS and SmS@Y_2O_2S [14]. Thus, the conditions found for the stabilization of oxide and sulfide phases during the synthesis of compounds Y_2O_3@SmS, $(Y_{0.90}Gd_{0.10})_2O_3$@SmS and $(Y_{0.99}Gd_{0.01})_2O_3$@SmS allowed us to achieve optimal values of the Seebeck coefficient in accordance with the formula for calculating the thermoelectric ZT parameter of material $ZT = S^2T/\rho\kappa_{\text{tot}}$.

At the same time, in the considered objects under study the tendency for increase in the resistivity of the material with increase in the thermo-emf index remains. Figure 3, b shows that for compounds Y_2O_3@SmS, $(Y_{0.90}Gd_{0.10})_2O_3$@SmS and $(Y_{0.99}Gd_{0.01})_2O_3$@SmS the parameter ρ achieved values of 9 to 17 $\mu\Omega\cdot$m at $T = 873$ K. The obtained values ρ are close to values

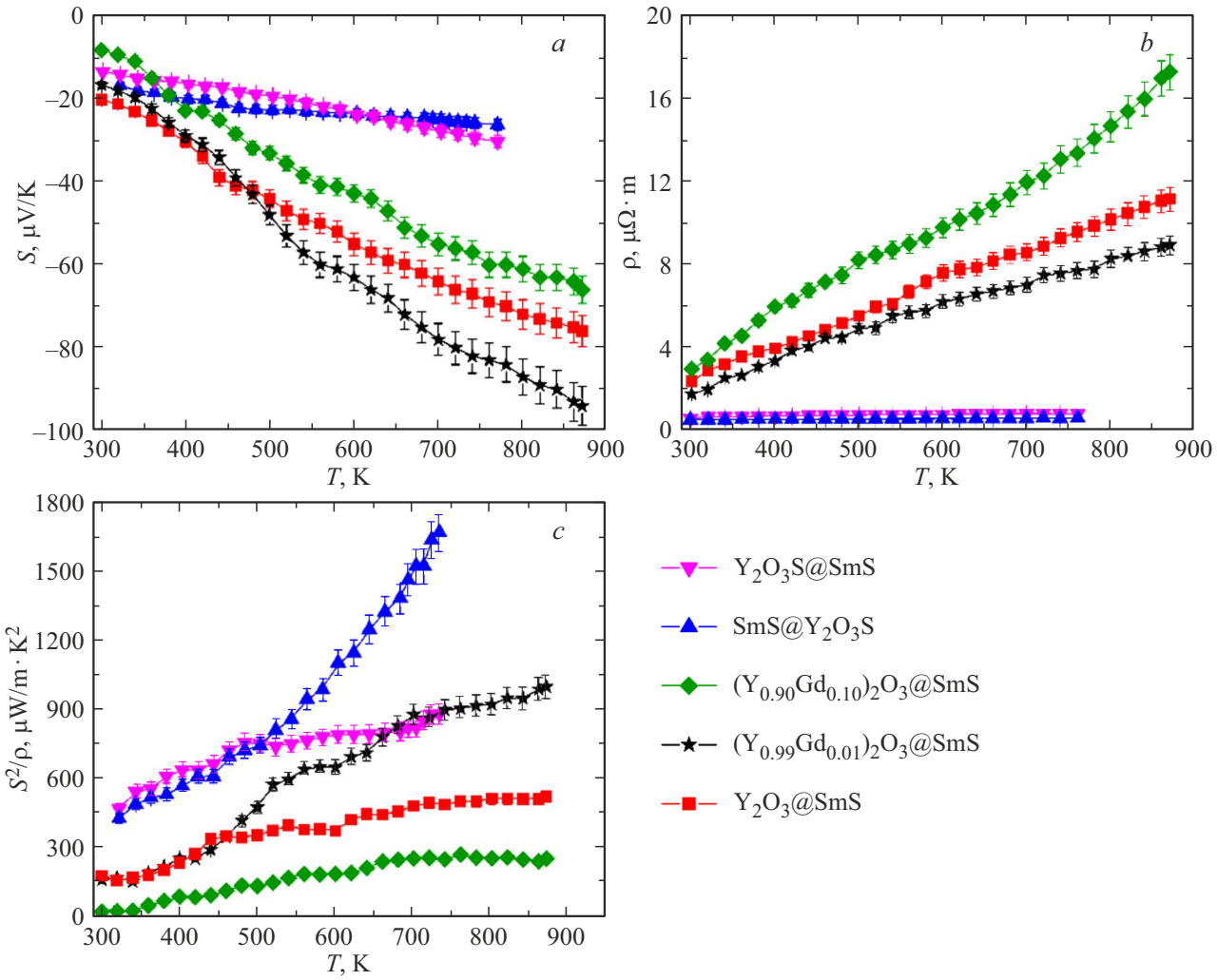

Figure 3. Temperature dependences: *a* — Seebeck coefficient S, *b* — resistivity ρ and *c* — power factor S^2/ρ for compounds Y_2O_3@SmS, $(Y_{0.90}Gd_{0.10})_2O_3$@SmS and $(Y_{0.99}Gd_{0.01})_2O_3$@SmS and comparison with previously obtained results for Y_2O_2S@SmS and SmS@Y_2O_2S [14].

obtained for previously studied compounds of compositions γ-$Ln_{0.8}Yb_{0.2}S_{1.5-y}$ ($20\,\mu\Omega\cdot$m at $T = 750$ K) with defect crystal lattice of Th_3P_4 type [18]. But the achieved here values ρ by order of magnitude are higher the values obtained in paper [14] for Y_2O_2S@SmS and SmS@Y_2O_2S (0.74 and $0.53\,\mu\Omega\cdot$m at $T = 773$ K). Also note that a slight increase in the resistivity with temperature increasing indicates a metallic type of conductivity in the compounds under study Y_2O_3@SmS, $(Y_{0.90}Gd_{0.10})_2O_3$@SmS and $(Y_{0.99}Gd_{0.01})_2O_3$@SmS.

Thus, the obtained high values of the Seebeck coefficient and optimal values of resistivity made it possible to achieve the values of the power factor $(S^2/\rho) \approx 995\,\mu$W/m · K at $T = 873$ K for compound $(Y_{0.99}Gd_{0.01})_2O_3$@SmS. This is the highest value among similar parameters S^2/ρ for considered in this paper compounds Y_2O_3@SmS, $(Y_{0.90}Gd_{0.10})_2O_3$@SmS and $(Y_{0.99}Gd_{0.01})_2O_3$@SmS. However, this value is lower than the obtained values of the parameter S^2/ρ in paper [14] for compounds Y_2O_2S@SmS and SmS@Y_2O_2S. In connection with this, it was interesting to study and compare the thermophysical properties of these compounds.

Figure 4 shows the temperature dependences of the overall thermal conductivity coefficient of the compounds Y_2O_3@SmS, $(Y_{0.90}Gd_{0.10})_2O_3$@SmS and $(Y_{0.99}Gd_{0.01})_2O_3$@SmS, Y_2O_2S@SmS and SmS@Y_2O_2S.

The value of the thermal conductivity coefficient was determined by the known equation $\kappa_{tot} = \chi_T DC_p$, where D — density of the ceramic sample, χ_T — temperature conductivity coefficient, and C_p — heat capacity of the material. With temperature increasing the increase in the parameter κ_{tot} is observed, and the thermal conductivity coefficient itself reaches values of 1.50−2.45 W/m · K. For composition $(Y_{0.99}Gd_{0.01})_2O_3$@SmS the minimum vaues of thermal conductivity coefficient $\kappa_{tot} = 1.50$ W/m · K is achieved at $T = 873$ K, this approximately by 2−3 times is lower then the same index for previously studied compounds Y_2O_2S@SmS and SmS@Y_2O_2S. Note that the

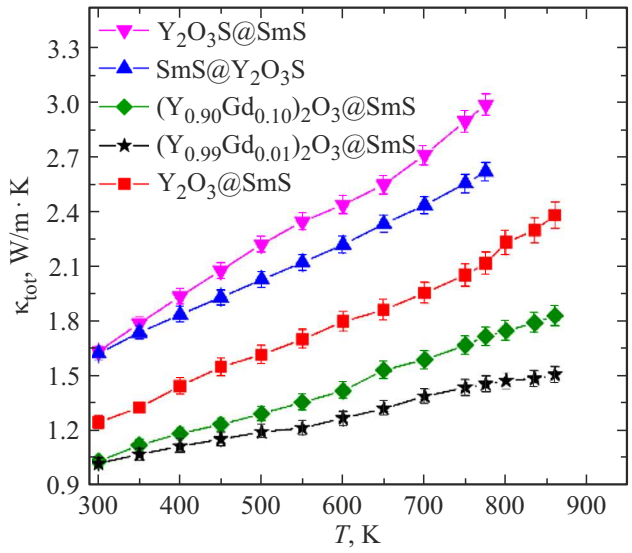

Figure 4. Temperature dependences of thermal conductivity coefficient κ_{tot} for compunds Y_2O_3@SmS, $(Y_{0.90}Gd_{0.10})_2O_3$@SmS and $(Y_{0.99}Gd_{0.01})_2O_3$@SmS and comparison with previously obtained results for Y_2O_2S@SmS and SmS@Y_2O_2S [14].

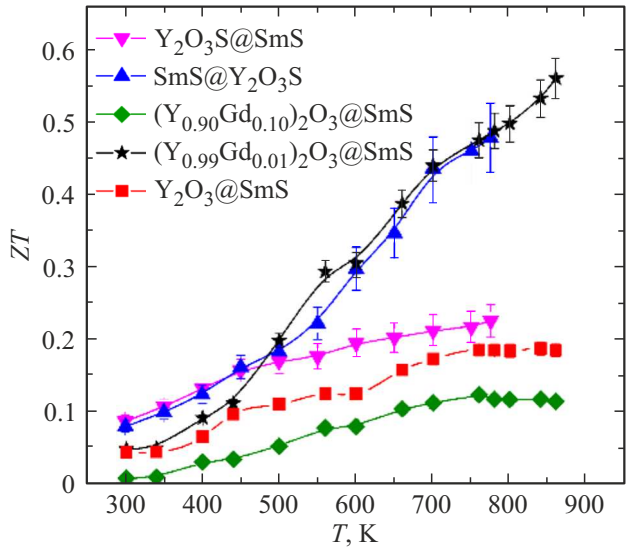

Figure 5. Temperature dependences of thermoelectric ZT parameter of studied compounds Y_2O_3@SmS, $(Y_{0.90}Gd_{0.10})_2O_3$@SmS and $(Y_{0.99}Gd_{0.01})_2O_3$@SmS and comparison with previously obtained results for Y_2O_2S@SmS and SmS@Y_2O_2S [14].

obtained thermal conductivity coefficient for the compound Y_2O_3@SmS at $T = 873$ K is $\kappa_{tot} = 2.35$ W/m · K. This is by $\sim 20\%$ lower then values κ_{tot} in compounds Y_2O_2S@SmS and SmS@Y_2O_2S. Thus, in this paper we obtained the compounds Y_2O_3@SmS, $(Y_{0.90}Gd_{0.10})_2O_3$@SmS and $(Y_{0.99}Gd_{0.01})_2O_3$@SmS with decreased thermal conductivity coefficient. The reason for this effect may be the introduction of a small amount of ions Gd^{3+} in sublattice Y_2O_3. This resulted in the creation of additional phonon scattering centers [19] and, as a consequence, in a further decrease in the thermal conductivity coefficient. As a result the obtained values κ_{tot} for compounds $(Y_{0.90}Gd_{0.10})_2O_3$@SmS and $(Y_{0.99}Gd_{0.01})_2O_3$@SmS at $T = 873$ K are 1.84 and 1.50 W/m · K, respectively. On the other hand, the results for parameter κ_{tot} by 1.5 times exceed the same values for compounds γ-$Ln_{0.8}Yb_{0.2}S_{1.5-y}$ with a cubic crystal lattice of Th_3P_4 type [18]. This is worth paying special attention to and looking for further ways to reduce the parameter κ_{tot} to increase the efficiency of the thermoelectric material. In the general case, the thermal conductivity coefficient includes two components and can be calculated using the formula $\kappa_{tot} = \kappa_{lat} + \kappa_{el}$, where κ_{lat} and κ_{el} — lattice and electronic components of thermal conductivity. Considering the low resistivity (high concentration of charge carriers) in the compounds under study Y_2O_3@SmS, $(Y_{0.90}Gd_{0.10})_2O_3$@SmS and $(Y_{0.99}Gd_{0.01})_2O_3$@SmS, it is necessary to take into account that the contribution of the electronic component of thermal conductivity will exceed 10%.

Figure 5 shows the temperature dependences of the thermoelectric ZT parameter of studied compounds Y_2O_3@SmS, $(Y_{0.90}Gd_{0.10})_2O_3$@SmS and $(Y_{0.99}Gd_{0.01})_2O_3$@SmS, and comparison with literature data, obtained for compounds Y_2O_2S@SmS and SmS@Y_2O_2S with core–shell nanostructure.

The obtained maximum value of thermoelectric ZT parameter of sample $(Y_{0.99}Gd_{0.01})_2O_3$@SmS at $T = 873$ K is $ZT = 0.56$, this is by ~ 3 times higher than the appropriate value for samples Y_2O_3@SmS ($ZT = 0.18$ at $T = 873$ K) and Y_2O_2S@SmS ($ZT = 0.23$ at $T = 773$ K). As can be seen from Figure 5, the temperature dependences for compounds SmS@Y_2O_2S and $(Y_{0.99}Gd_{0.01})_2O_3$@SmS are characterized by close parameter values ZT. This is primarily caused by a lower parameter in the compound SmS@Y_2O_2S and by higher resistivity in the sample $(Y_{0.99}Gd_{0.01})_2O_3$@SmS. On the other hand, the obtained temperature dependences of the thermal conductivity coefficient for compounds containing ions Gd^{3+} demonstrate low values of the parameter κ_{tot} in comparison with similar data for compounds Y_2O_2 S@SmS and SmS@Y_2O_2S. Thus, it is necessary to continue to look for ways to optimize the thermoelectric properties of compounds with core-shell nanostructures to achieve higher parameter values ZT. It is obvious that further steps to increase the efficiency of the thermoelectric material shall be associated with the optimization of compositions in the „core“ and „shell“ subsystems — the creation of solid solutions, as well as the use of rare earth metals with larger difference in ionic radii.

4. Conclusion

Based on the results of this paper, a series of samples was synthesized based on rare earth elements, their oxides and monosulfides with compositions Y_2O_3@SmS, $(Y_{0.90}Gd_{0.10})_2O_3$@SmS and $(Y_{0.99}Gd_{0.01})_2O_3$@SmS with core–shell nanostructure. The synthesis included multi-

stage processes using the polyol sol-gel method, sulfidation and high-temperature annealing with the search and establishment of optimal synthesis times and temperatures to stabilize the oxide and monosulfide phases. It was determined that the compounds exhibit promising thermoelectric properties at elevated temperatures up to $T = 873\,\mathrm{K}$ and above. For the compound $(Y_{0.99}Gd_{0.01})_2O_3$@SmS at $T = 873\,\mathrm{K}$ the values of the main thermoelectric parameters are achieved: Seebeck coefficient $S = -94\,\mu\mathrm{V/K}$, resistivity $\rho = 17\,\mu\Omega$ and total thermal conductivity coefficient $\kappa_{\mathrm{tot}} = 1.50\,\mathrm{W/m \cdot K}$. At that the maximum thermoelectric ZT parameter of compound $(Y_{0.99}Gd_{0.01})_2O_3$@SmS achieves values $ZT = 0.56$ at $T = 873\,\mathrm{K}$, which is a competitive and promising result in comparison with other thermoelectric materials based on REE.

To further thermoelectric ZT parameter increasing and obtaining the effective thermoelectric material with core-shell nanostructure, it is necessary to optimize the compositions, the optimization consists in obtaining solid solutions based on oxides and monosulfides of rare earth elements using REM with a large difference in ionic radii. This, to a large extent, will make it possible to complicate the phonon spectrum of compounds and to reduce the thermal conductivity of the material, as well as to increase the power factor of the thermoelectric material. Thus, it will be possible to obtain a high-temperature thermoelectric device corresponding to the concept of phononic glass-electron crystal with a core-shell nanostructure.

Acknowledgments

The authors of the article express their gratitude to T.D. Pivovarova (IChI SB RAS) for assistance in the synthesis of the compounds under study and Ph.D. E.Yu. Gerasimov (Institute of Catalysis of SB RAS) for obtaining the experimental results of HRTEM. The authors thank the Ministry of Science and Higher Education of the Russian Federation (project № 121031700315-2).

Funding

This study was supported by a grant from the Russian Science Foundation № 22-73-00013.

Conflict of interest

The authors declare that they have no conflict of interest.

References

[1] M. Mukherjee, A. Srivastava, A.K. Singh. J. Mater. Chem. C **10**, *35*, 12524 (2022).
[2] S.M. Pourkiaei, M.H. Ahmadi, M. Sadeghzadeh, S. Moosavi, F. Pourfayaz, L. Chen, M.A. Pour Yazdi, R. Kumar. Energy **186**, *c*, 115849 (2019).
[3] H. Zhu, C. Xiao. Front. Phys. **13**, *3*, 137202 (2018).
[4] M. Zebarjadi, K. Esfarjani, M.S. Dresselhaus, Z.F. Ren, G. Chen. Energy Environ. Sci. **5**, *1*, 5147 (2012).
[5] W. Bou Nader. Appl. Therm. Eng. **167**, 114761 (2020).
[6] W. Ren, Y. Sun, D. Zhao, A. Aili, S. Zhang, C. Shi, J. Zhang, H. Geng, J. Zhang, L. Zhang, J. Xiao, R. Yang. Sci. Adv. **7**, *7*, 22 (2021).
[7] M.M. Alsalama, H. Hamoudi, A. Abdala, Z.K. Ghouri, K.M. Youssef. Rev. Adv. Mater. Sci. **59**, *1*, 371 (2020).
[8] G.J. Snyder, E.S. Toberer. Nature Mater. **7**, *2*, 105 (2008).
[9] G.J. Snyder. Appl. Phys. Lett. **84**, *13*, 2436 (2004).
[10] M. Hamid Elsheikh, D.A. Shnawah, M.F.M. Sabri, S.B.M. Said, M. Haji Hassan, M.B. Ali Bashir, M. Mohamad. Renew. Sustain. Energy Rev. **30**, *C*, 337 (2014).
[11] D.K. Aswal, R. Basu, A. Singh. Energy Convers. Manag. *114*, 50 (2016).
[12] C. Gayner, K.K. Kar. Prog. Mater. Sci. **83**, 330 (2016).
[13] S. LeBlanc. Sustain. Mater. Technol. **1–2**, 26 (2014).
[14] A.V. Sotnikov, V.V. Bakovets, E.V. Korotaev, M.M. Syrokvashin, A.S. Agazhanov, D.P. Pishchur. Chem. Phys. Lett. **809**, 140157 (2022).
[15] A.V. Sotnikov, P. Jood, M. Ohta. ACS Omega **5**, *22*, 13006 (2020).
[16] V.V. Bakovets, A.V. Sotnikov, A.S. Agazhanov, S.V. Stankus, E.V. Korotaev, D.P. Pishchur, A.I. Shkatulov. J. Am. Ceram. Soc. **101**, **10**, 4773 (2018).
[17] A.V. Golubkov, M.M. Kazanin, V.V. Kaminskii, V.V. Sokolov, S.M. Solov'ev, L.N. Trushnikova. Inorg. Mater. **39**, *12*, 1251 (2003).
[18] A.V. Sotnikov, M.M. Syrokvashin, V.V. Bakovets, I.Yu. Flatova, E.V. Korotaev, A.Sh. Agazhanov, D.A. Samoshkin. J. Am. Ceram. Soc. **105**, *4*, 2813 (2022).
[19] A.V. Sotnikov, V.V. Bakovets, M. Ohta, A.Sh. Agazhanov, S.V. Stankus. Phys. Solid State **62**, *4*, 611 (2020).
[20] A.V. Sotnikov, V.V. Bakovets, A.Sh. Agazhanov, S.V. Stankus, D.P. Pishchur, V.V. Sokolov. Phys. Solid State **60**, *3*, 487 (2018).
[21] J. He, M.G. Kanatzidis, V.P. Dravid. Mater. Today **16**, *5*, 166 (2013).
[22] A.V. Shevelkov. Russ. Chem. Rev. **77**, *1*, 1 (2008).
[23] W. Liu, Q. Jie, H.S. Kim, Z. Ren. Acta Mater. **87**, 357 (2015).
[24] A.V. Sotnikov, V.V. Bakovets, M.M. Syrokvashin, I.Yu. Filatova. Inorg. Mater. **58**, *10*, 1105 (2022).
[25] A.V. Sotnikov, M.M. Syrokvashin, V.V. Bakovets, E.V. Korotaev, E.Yu. Gerasimov. Chem. Phys. Lett. **826**, 140636 (2023).
[26] M. Ohta, H. Yuan, S. Hirai, Y. Yajima, T. Nishimura, K. Shimakage. J. Alloys. Compd **451**, *1–2*, 627 (2008).
[27] M. Ohta, S. Hirai, H. Kato, V.V. Sokolov, V.V. Bakovets. Mater. Trans. **50**, *7*, 1885 (2009).

Translated by I.Mazurov